

Article

# Structure of Rhodolith Beds and Surrounding Habitats at the Doce River Shelf (Brazil)

Vitória L. Holz<sup>1</sup>, Ricardo G. Bahia<sup>1,\*</sup> , Cláudia S. Karez<sup>1</sup> , Fernanda V. Vieira<sup>2</sup>,  
Fernando C. Moraes<sup>1</sup>, Nicholas F. Vale<sup>1</sup>, Daniela B. Sudatti<sup>1</sup>, Leonardo T. Salgado<sup>1</sup>,  
Rodrigo L. Moura<sup>3</sup> , Gilberto M. Amado-Filho<sup>1</sup> and Alex C. Bastos<sup>2</sup> 

<sup>1</sup> Rio de Janeiro Botanical Garden Research Institute, Rua Pacheco Leão 915, Rio de Janeiro, RJ 22460-030, Brazil; vitoriaholz@gmail.com (V.L.H.); claudia.karez@gmail.com (C.S.K.); fmoraes@mn.ufrj.br (F.C.M.); nicholasdovale@gmail.com (N.F.V.); dbsudatti@id.uff.br (D.B.S.); lsalgado.jbrj@gmail.com (L.T.S.); gilbertoamadofilho@gmail.com (G.M.A.-F.)

<sup>2</sup> Department of Oceanography, Federal University of Espírito Santo (UFES), Avenida Fernando Ferrari 514, Vitória, ES 29090-600, Brazil; fernanda.vedoato@gmail.com (F.V.V.); alexcardosobastos@gmail.com (A.C.B.)

<sup>3</sup> Institute of Biology and SAGE-COPPE, Federal University of Rio de Janeiro (UFRJ), Rio de Janeiro, RJ 21941-599, Brazil; moura.uesc@gmail.com

\* Correspondence: ricardo.bahia@gmail.com

Received: 29 January 2020; Accepted: 12 February 2020; Published: 15 February 2020



**Abstract:** The world's largest rhodolith beds have been reported from the Brazilian continental shelf. Highly biodiverse beds are located in Southeast Brazil, but ecological aspects of these beds remain unknown. Despite their ecological importance, rhodolith beds (RBs) have recently been subjected to a severe threat, when more than 35 million cubic meters of mining residues slid down a mountainside on 5 November 2015, after a collapse of a gigantic dam upstream (the Mariana disaster), causing a huge impact on the Doce River. Our aim is to assess rhodolith beds and adjacent coralline formations on the Doce River Shelf (DRS) after the dam collapse. This paper describes the distribution, abundance, vitality, size and shape, as well as unmapped bryozoan rich sediment formations in this area, serving as baseline knowledge for environmental monitoring. Four distinct biogenic sea bottom habitats (bryozoan bottoms, rhodolith beds, carbonate concretions, and reefs) were recognized at different depth ranges with distribution indicated to be mostly related to the local sedimentary regime. Mud sediments dominated the seafloor up to 35 m depth. On the mid shelf, bryozoan bottoms were recorded from 35 to 45 m depth. Crustose coralline algae (CCA) occurring as rhodoliths and carbonate concretions extend over 1953 km<sup>2</sup> in the mid and outer shelf. Rhodolith beds predominate in these areas, totaling 1521 km<sup>2</sup> of sea bottom and were more abundant at depths between 45 and 65 m, occupying an extensive area south of the Doce River mouth. Northward, rhodolith beds are less abundant or absent likely due to the long-term deposition of fine sediments in this region. Carbonate concretions and reefs covered by CCA occupy sparse areas on the outer shelf (65–105 m depth). Differences in rhodolith features recorded, including coverage, density and size, may be related to the Doce River sedimentation and related factors (e.g., hydrodynamics, depth, and light). However, since there are no previous detailed studies on RBs along the DRS, we could not assess the impact of sedimentation of dam wastes on RBs' abundance and density. In any case, these are valuable results for the further monitoring of long-term effects. Considering that the growth of these rhodoliths is relatively slow, and that they are affected by the sedimentation from the Doce River, the implementation of a management and conservation plan for this area is necessary in order to preserve this ecosystem.

**Keywords:** carbonate reefs; rhodolith beds; coralline algae; mesophotic habitat; Bryozoa; Espírito Santo Continental Shelf

## 1. Introduction

Rhodoliths are free-living nodules composed mostly (>50%) of non-geniculate coralline algae [1]. They require water motion (waves and currents) or bioturbation to be kept in an unattached and unburied state [2]. They can be aggregated, giving rise to rhodolith beds (RBs), which are identified and delimited as areas with more than 10% cover of live rhodoliths over a minimum area of 500 m<sup>2</sup> [3]. Rhodoliths are classified into three morphological groups with different internal structures: compact and nodular pralines, larger and vacuolar boxwork rhodoliths, and unattached branches [3–5]. Each of the three morphological groups correspond to a group of composing coralline species and associated biota and are possibly correlated with environmental variables, including hydrodynamics and sedimentation [3].

Rhodolith beds increase the structural complexity of the seabed in comparison with soft sediments, thus providing more space, nurseries, refuges, and resources for cryptofauna, macroalgae, and fishes, and thus enhancing species richness and abundance [2]. Other important ecosystem services provided by RBs are calcium carbonate production, carbon sequestration, and fisheries [6]. Their abundance, size, and shape can vary in space and time and also under anthropogenic impacts (e.g., rhodolith extraction, trawling; [2]) and their carbonate production by climate change (e.g., acidification and elevated temperature; [7–9]). Although there are exploitations of RBs in some areas, they are recognized as a nonrenewable resource that is threatened by human activities and that represents critical habitat for biodiversity conservation [10,11].

The assessment of RBs for monitoring studies should include, besides the location and areal extent, the occurrence of macroscopic sedimentary structures on the bottom, the mean percentage cover of live thalli and surface live/dead ratio, the coverage of dominant the morphologies of rhodoliths, and the identification of important non-geniculate coralline algae species [3]. In addition to rhodoliths, crustose coralline algae (CCA) may overgrow on hard and relatively flat substrates, forming concretions named henceforth as carbonate concretions [12] or CCA concretions. Both CCA forms should be recorded separately in monitoring studies as they represent different habitats and may compete with each other.

The world's largest RBs were reported in the Brazilian Continental Shelf, where they represent a major marine habitat over extensive and continuous areas from 2° N to 23° S, encompassing the mid- to outer- shelf (30–120 m depth) and surrounding oceanic islands [6]. Several aspects about these beds have been investigated such as, for example, their distribution, mapping, associated organisms, coralline species composition, and internal structure [6,13–18]. RBs and carbonate reefs off the Amazon River mouth have recently drawn international attention because of their high associated biodiversity coupled with their proximity to allotments of Oil and Gas block exploration fields in the Brazilian Equatorial Margin [18,19]. Despite advanced knowledge and increased threat, most RBs in the Brazilian continental shelf remain poorly studied concerning ecological aspects (e.g., rhodolith coverage, size, shape) that are crucial for monitoring, conservation, and management purposes.

The Espírito Santo Continental Shelf (ESCS) in the Southwestern Atlantic (Brazil) is dominated by carbonate sand/gravel beds and extensive RBs [20]. At the ESCS, RBs provide an important habitat for epibenthic communities [13,21,22], supporting endemic species such as the macroalgae *Laminaria abyssalis* [23]. The ESCS central zone is mainly influenced by the discharge of the Doce River, one of the largest rivers in Southeastern Brazil. This zone is herein referred to as the Doce River Shelf (DRS). More than 35 million cubic meters of mining residues slid down a mountainside on 5 November 2015, after a collapse of a gigantic dam upstream (the Mariana disaster), causing a huge impact on the Doce River. On 21 November 2015, mining wastes reached the coastal marine ecosystem, 17 days after the disaster of Mariana city. About 74 million tons of sediment were discharged into the ocean during the 14 months following the dam collapse (November 2015–December 2016; [24]). Its short-term impacts included rapid sedimentation burying the photosynthetic organisms and surficial benthic assemblages, causing mortality of sessile organisms and altering processes such as bioturbation [25], thus affecting the distributions of RBs [24]. Other factors could also have serious effects on the rhodolith vitality, including the increase of water turbidity and metal contamination in water/sediments [26].

In this sense, our aim was to describe the rhodolith beds and surrounding habitats at the DRS after the dam collapse. Specifically, we aimed to assess rhodolith abundance (% cover), density (rhodoliths·m<sup>-2</sup>), vitality, size and shape as well as undescribed surrounding bryozoan bottoms, carbonate concretions and reefs along a depth gradient from 35 to 105 m at the DRS.

## 2. Materials and Methods

### 2.1. Study Area

The Doce River Shelf (DRS; 17°53' S–22°18' S) is located in the central zone of the ESCS (Figure 1). The Doce River is the main source of fresh water and sediments for the area, with an average discharge volume of 700 m<sup>3</sup>/s/year and sediment load of 603,106 ton/year [27]. The sedimentation pattern in the adjacent area of the Doce River mouth is directly influenced by the river sediment supply and it is a result of fluvial and meteoceanographic conditions [28]. A seabed sedimentary facies distribution map of DRS was produced by Bastos et al. [20]. A riverine terrigenous mud deposit is located in the inner shelf, which is characterized by a deltaic lobe ending at 30 m water depth. Towards offshore, in the outer shelf, the seabed morphology becomes flatter with a transition to sandy facies while an increase in carbonate content is observed deeper than 40 m, where RBs are dominant [20].

The DRS area includes two contiguous national Marine Protected Areas (MPAs): One of sustainable use (Costa das Algas Environmental Protection Area) and one no-take area (Santa Cruz National Wildlife Refuge), both created on 17 June 2010 to conserve the richest macroalgae flora in Brazil [29,30]. This high biodiversity has been associated with RBs extending from depths greater than 40 m down to 100 m [13,20,21,30,31].

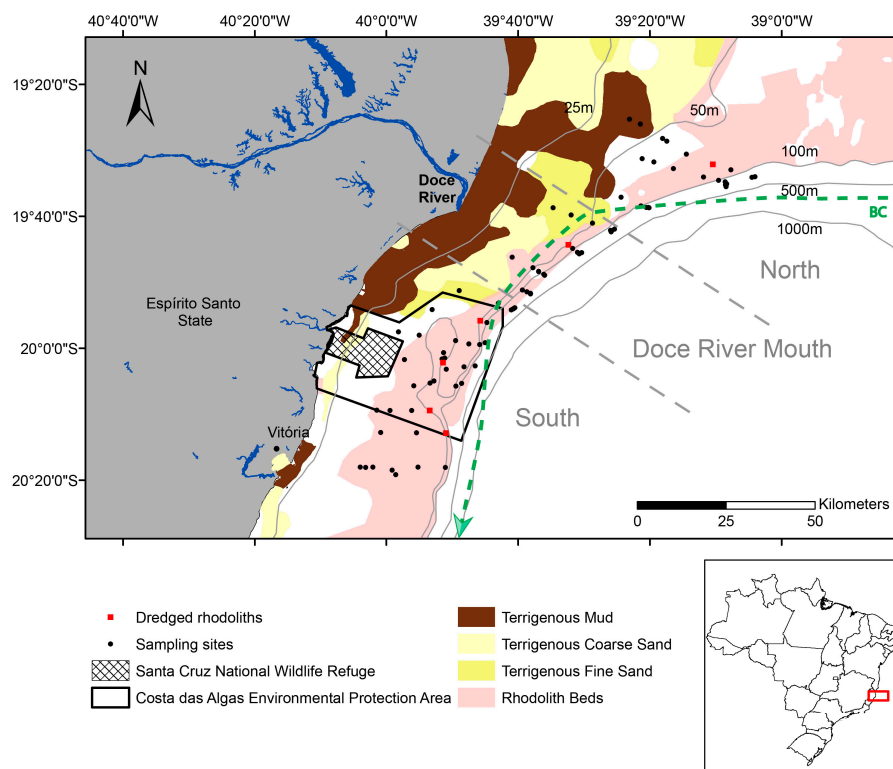


**Figure 1.** Sampling sites at the RBs on Doce River Shelf (DRS) from 35 to 105 m depth, located at the three zones: North, Doce River Mouth, and South. Polygons (the hatched one and the black one) indicate the two National Marine Protected Areas in the study area. Data of sedimentary facies and dominant marine current, i.e., Brazil Current (BC, green dashed line), were obtained from Bastos et al. [20], and Vieira et al. [32]. Datum: WGS1984.

## 2.2. Rhodolith Sampling and Characterization

Based on the RBs' delimitation at ESCS [20,32], 15 transects were placed perpendicularly to the shoreline from 35 to 105 m depth, within the DRS, totalling 88 sampling sites (Figure 1). At each site, a drop camera was used to capture seabed images. The drop camera was composed of a stainless-steel pyramidal frame with two GoPro Hero 4 Black cameras inserted in customized housings, one facing down (orthogonal) to a 60 × 60 cm quadrat and the other facing forward, both illuminated by flashlights. At each sampling site, 5–8 drop camera landings were performed to record orthogonal images that were used as photo-quadrats. The cameras recorded videos in ultra definition (4K format), from which still frames were extracted, providing 4000 × 3000 pixel and 72 dpi images. In addition, rhodoliths were sampled using a rectangular dredge in six different sites from 50 to 65 m depth to record size and to identify rhodolith-forming coralline algae species (Figure 1). The area was sampled during two expeditions, one on 18 December 2015 and another during April/May 2017. Supplementary qualitative imagery was produced on December 2018 and February 2019.

The percent cover of rhodoliths and carbonate concretions was estimated using the software Coral Point Count with Excel extensions (CPCe; [33]) from the analysis of 50 random points distributed in each photo-quadrat. The percentage cover of crustose coralline algae, rhodoliths, and carbonate concretions were plotted in distribution maps generated in ArcGis software by ESRI (Environmental Systems Resource Institute, ArcMap 10.1, <https://www.esri.com/en-us/home>). Simplified classes of coverage were utilized based on these maps by considering the following classes: Very low (<10%), low ( $\geq 10\%$ ,  $\leq 30\%$ ), medium ( $>30\%$ ,  $\leq 50\%$ ), high ( $>50\%$ ,  $\leq 70\%$ ), and very high ( $>70\%$ ). Density of rhodoliths was estimated by counting the total number of individual nodules divided by the area occupied in each photo-quadrat (rhodoliths·m<sup>-2</sup>). The vitality (= % total rhodolith – % dead rhodolith) was determined based on the observation of rhodolith coloration (pink, purple, or reddish color) following Bahia et al. [34].

Rhodolith size (mean diameter) was determined using Image J software [35] to measure the longest and shortest axes of each nodule ( $n = 20$  rhodoliths randomly chosen in each photo-quadrat). These measurements provided an approximation of original rhodolith size since they were based on a bidimensional method. The rhodolith mean diameter was obtained from the mean of each rhodolith two axes ( $n = \sim 2000$ ). Rhodolith shape was determined from dredged material ( $n = 165$ ) in accordance with Bosence and Pedley [36], by plotting the long, intermediate, and short axes using the TRIPLLOT v.1.4-2 spreadsheet of Graham and Midgley [37], which separates rhodoliths into spheroidal, discoidal, or ellipsoidal shapes. In addition, using the dredged material, rhodoliths were classified based on their morphology (boxwork, praline, or branches) according to Basso [5] and Basso et al. [38], plotting the results in a ternary diagram.

The identification of coralline algae species on the external surfaces of rhodoliths was conducted using histological sections of fertile material following the methods described by Maneveldt and Van der Merwe [39]. The taxa were morpho-anatomically identified according to Bahia [40].

The variability in biotic parameters (percent cover, nodules density, and vitality) was evaluated from 36 to 105 m depth, considering each 10 m depth interval, by Permutational Multivariate ANOVA (PERMANOVA; [41]) with depth as fixed factor. Analyses were based on Bray–Curtis dissimilarities (percent cover and density). *P*-values were calculated from 4999 unrestricted permutations of the raw data. When appropriate, pairwise comparisons were used to detect differences among levels of significant factors ( $p < 0.05$ ). The statistical analyses were conducted using PRIMER (version 6) + PERMANOVA software [42].

## 3. Results

Four main biogenic formations were recognized at different depth ranges on the DRS: Bryozoan bottoms, rhodolith beds, carbonate concretions, and reefs (Figure 2). Down to the first 35 m in depth, the inner shelf sea bottom was composed mainly of mud/sand siliciclastic sediments. Towards offshore, a transition from medium/coarse sand to gravel was observed (Figure 3).

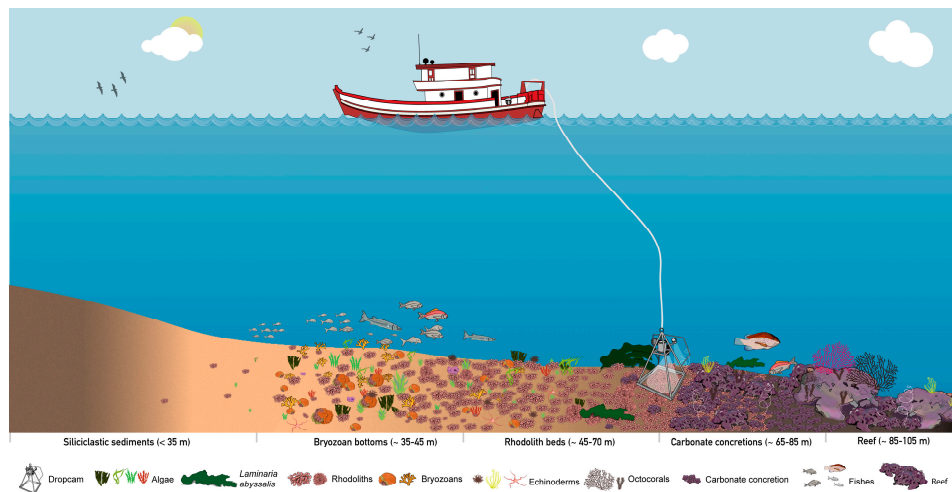


**Figure 2.** Illustrative representation showing sampling method with drop camera and the four main mesophotic biogenic habitats found on the sea bottom of the mid-outer Doce River Shelf (35–105 m depth). Size of objects in the figure are merely illustrative being disproportional and out of scale with regard to their original sizes.

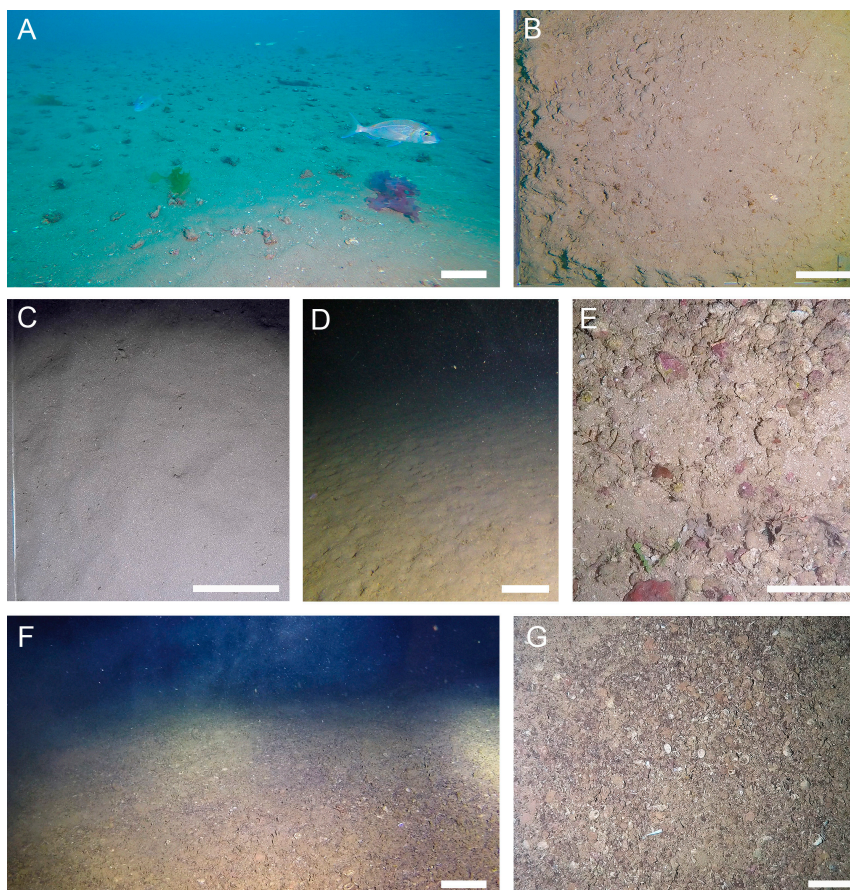


**Figure 3.** In situ images of sediment facies at different sampling sites/depths on the DRS (Table A1): (A) Sand bottom with sparsely distributed rhodoliths and macroalgae at DR5 (40 m); (B) Mud bottom at S7 (42 m); (C) Sand bottom at DR1 (60 m); (D) Mud bottom at DR4 (68 m); (E) Gravel bottom with crustose coralline algae (CCA), Bryozoa and *Halimeda* sp. at DR2 (80 m); (F,G) Panoramic and detailed view of gravel bottom at S6 (100 m), respectively. A, C, D, and F (lateral view); B, E, and G (orthogonal view). Scale bar = 10 cm.

On the mid shelf, the first biogenic habitat was formed by bryozoans and recorded from 35 to 45 m depth (Figure 4). Dozens of bryozoan species were recorded, including *Celleporaria atlantica* (erect robust branching), *Stylopoma hastata* (encrusting multilaminar), and *Metrarabdotos* sp. (erect delicate branching) as the most conspicuous ones. Bryozoan bottoms were recorded as patchy aggregations, where sponges, ascidians, and echinoderms (crinoids) find space to grow as conspicuous faunal components.

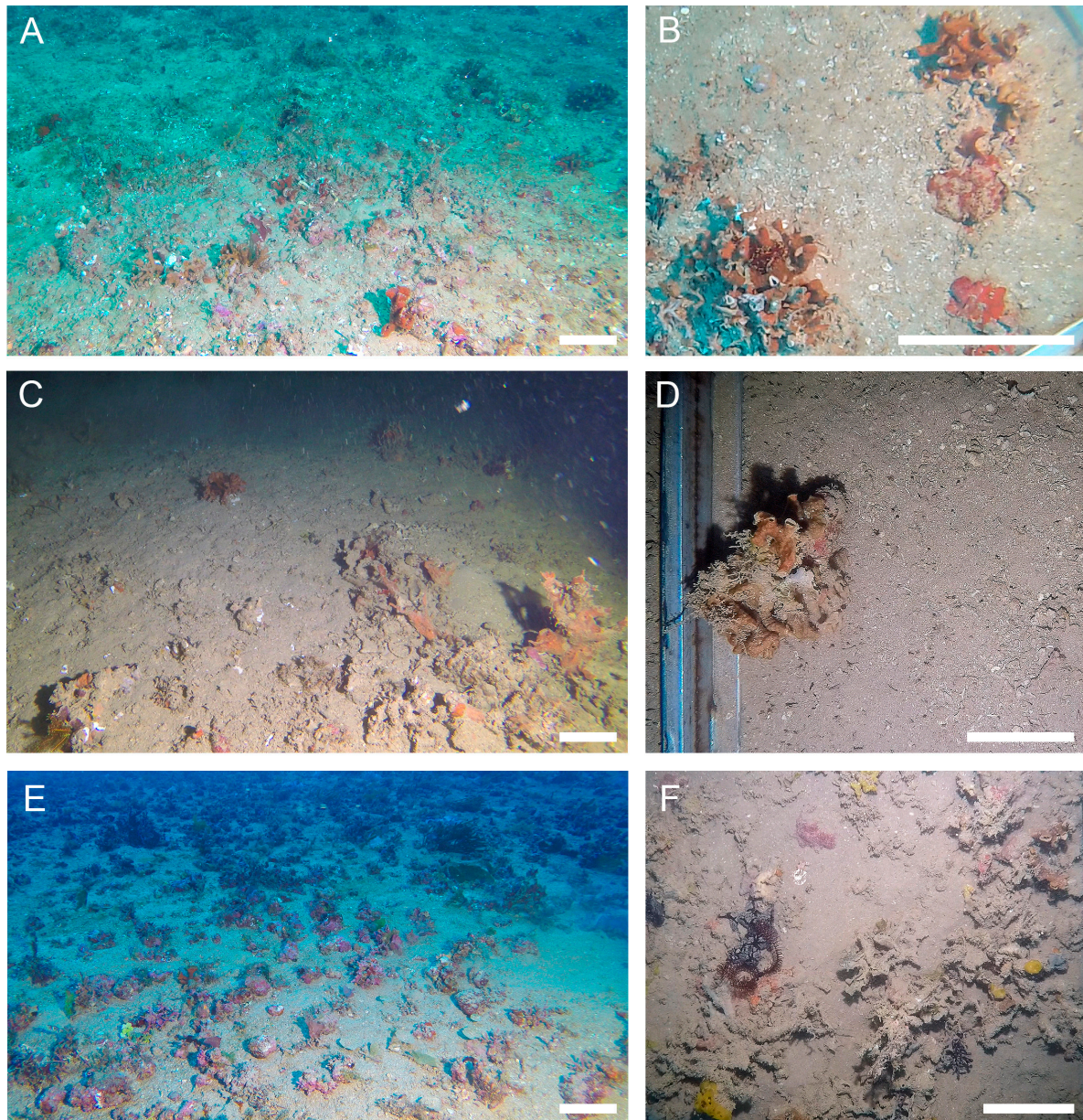


**Figure 4.** In situ images of Bryozoa bottoms at different sampling sites/depths on the DRS (Table A1): (A) *Celleporaria atlantica* colonies, ascidians (*Didemnum* sp.—white) and CCA at S7 (42 m); (B) detail of *C. atlantica* colonies and *Peyssonnelia* sp. at S9 (40 m); (C) Bryozoa colonies and sponges at S5 (45 m); (D) *C. atlantica* colony on sand at S3 (45 m); (E) Loose rhodoliths and bryozoans on sand bottom at S8 (49 m); (F) Bryozoa colonies (*C. atlantica* and *Metrarabdotos* sp.) partially covered by fine sediment at N1 (50 m). A, C, and E (lateral view); B, D, and F (orthogonal view). Scale bar = 10 cm.

The second and most extensive biogenic habitat was rhodolith beds, which occupied much of the mid/outer shelf, from 45 to 85 m depth, varying in density along the shelf and according to depth (Figures 5–7). The densest area (mean 90 rhodoliths·m<sup>-2</sup>) was recorded between 45 and 65 m depth,

located at Costa das Algas Environmental Protected Area at about 40 km from the Doce River mouth. In a general pattern, rhodolith beds become denser towards the shelf slope, showing a transition from sparse and loose nodules, interspersed by carbonate sand/gravel/bryozoans, to highly dense aggregates, where we suggest that rhodoliths become fused to each other to build carbonate concretions (Figure 8A–D).

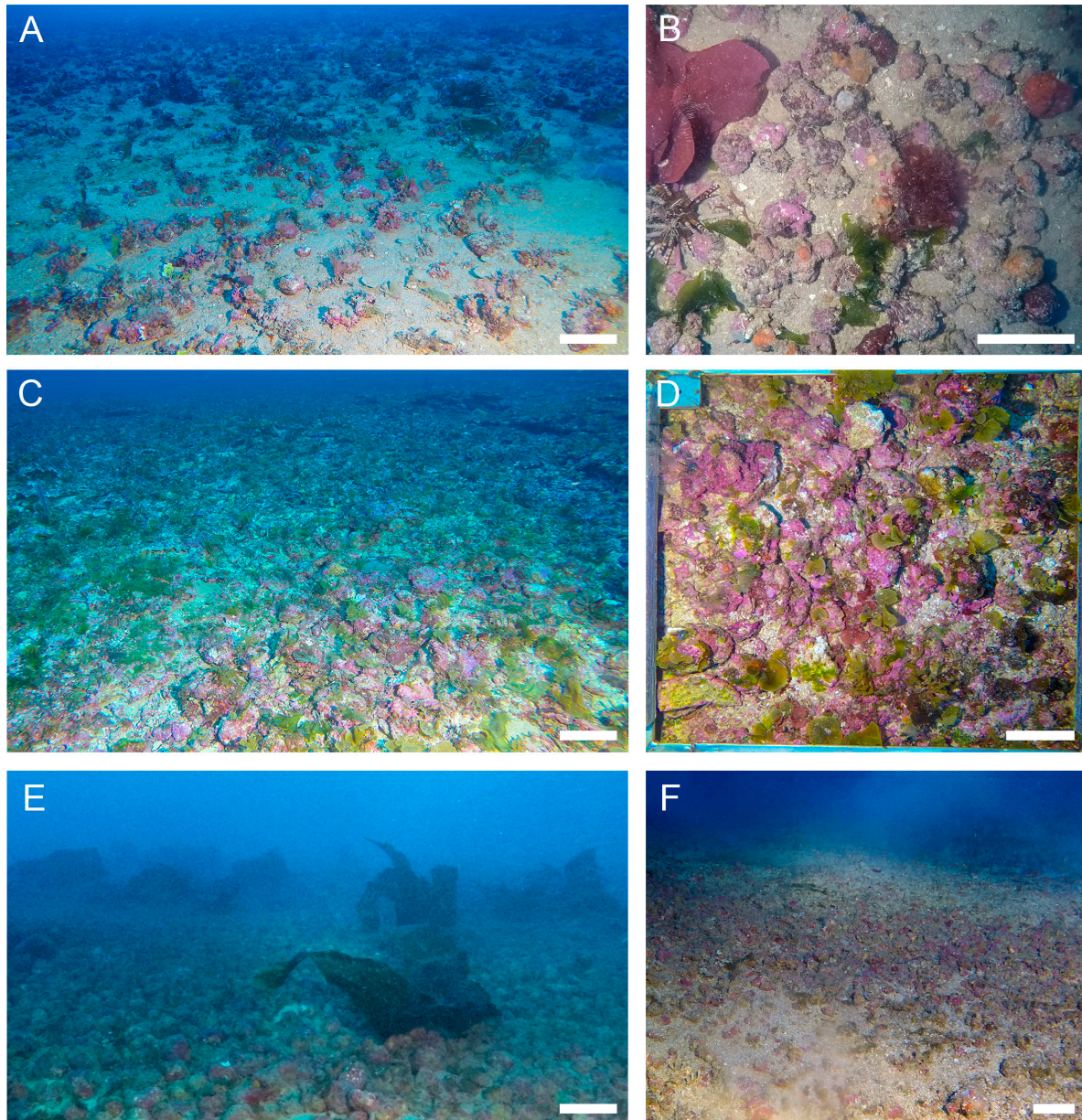


**Figure 5.** In situ images of rhodolith beds at different sampling sites/depths on the DRS (Table A1): (A) Rhodolith bed at S8 (49 m); (B) Loose rhodolith nodules with associated macroalgae and invertebrates at DR3 (50 m); (C) Densely distributed rhodoliths in transition to carbonate concretions at S4 (63 m); (D) High vitality rhodoliths and macroalgae at S4 (63 m); (E) Rhodolith bed harboring the endemic kelp (*Laminaria abyssalis*) at N3 (70 m); (F) Loose rhodoliths intermingled by coarse sediment at N4 (90 m). A, C, E, and F (lateral view); B and D (orthogonal view). Scale bar = 10 cm.

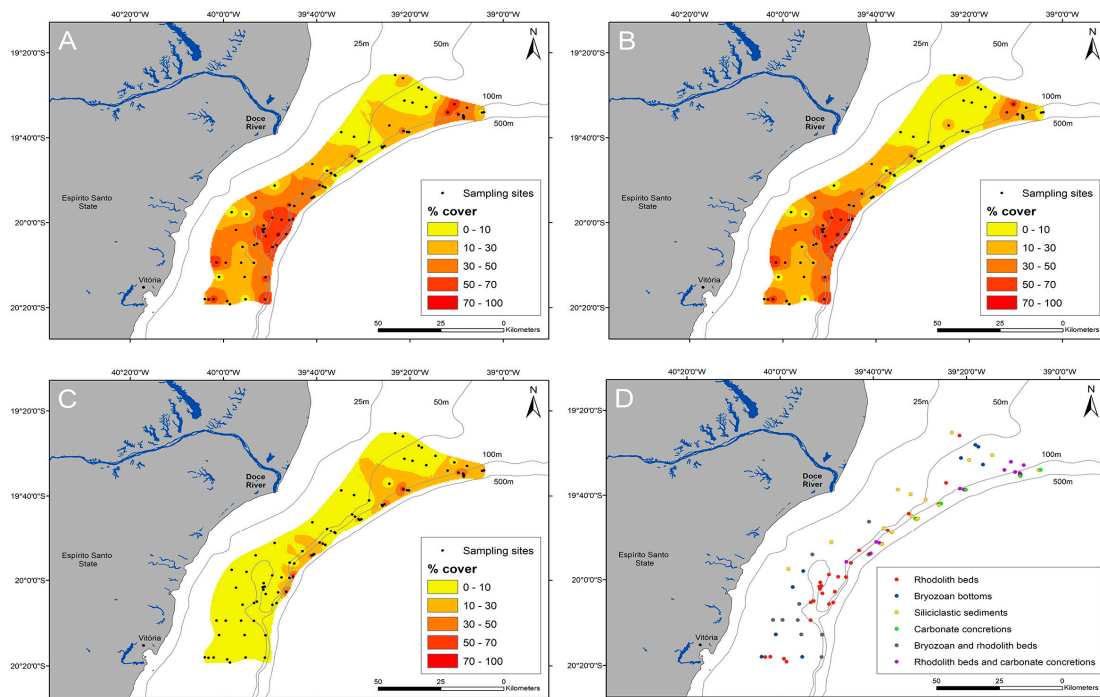


**Figure 6.** Distribution of biogenic formations at the mid-outer on the DRS: (A) Coralline crustose algae distribution, which includes both forms, rhodoliths (free-living nodules) and carbonate concretions; (B) Rhodolith distribution; (C) Carbonate concretion distribution; (D) Rhodolith beds, surrounding biogenic formations and siliciclastic sediments distribution captured by images at study sites. Datum: WGS1984. Maps were created using ArcGIS software by ESRI (Environmental Systems Resource Institute, ArcMap 10.1, <https://www.esri.com/en-us/home>).

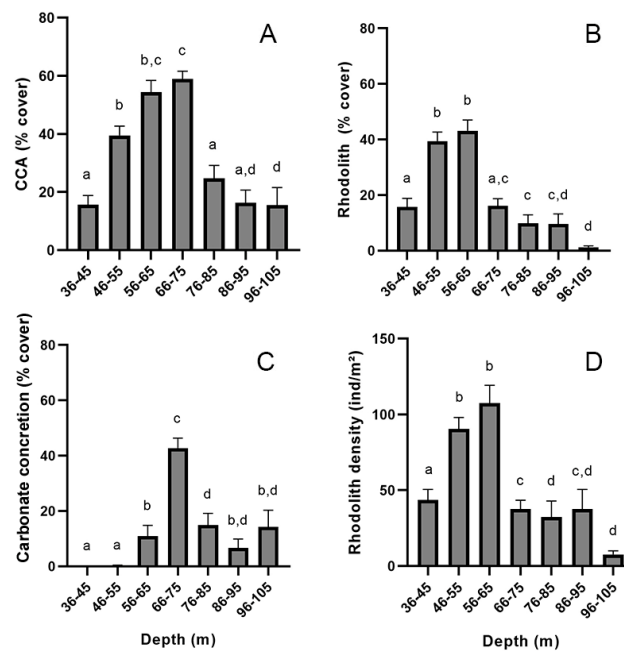


**Figure 7.** Coralline algae abundance at the Doce River Shelf (DRS) along the depth gradient from 35 to 105 m at each 10 m depth interval: (A) Coralline crustose algae percent cover which include both forms—rhodoliths and crustose algae concretions; (B) Rhodolith percent cover; (C) Carbonate concretion percent cover; (D) Rhodolith density (rhodoliths·m<sup>-2</sup>).

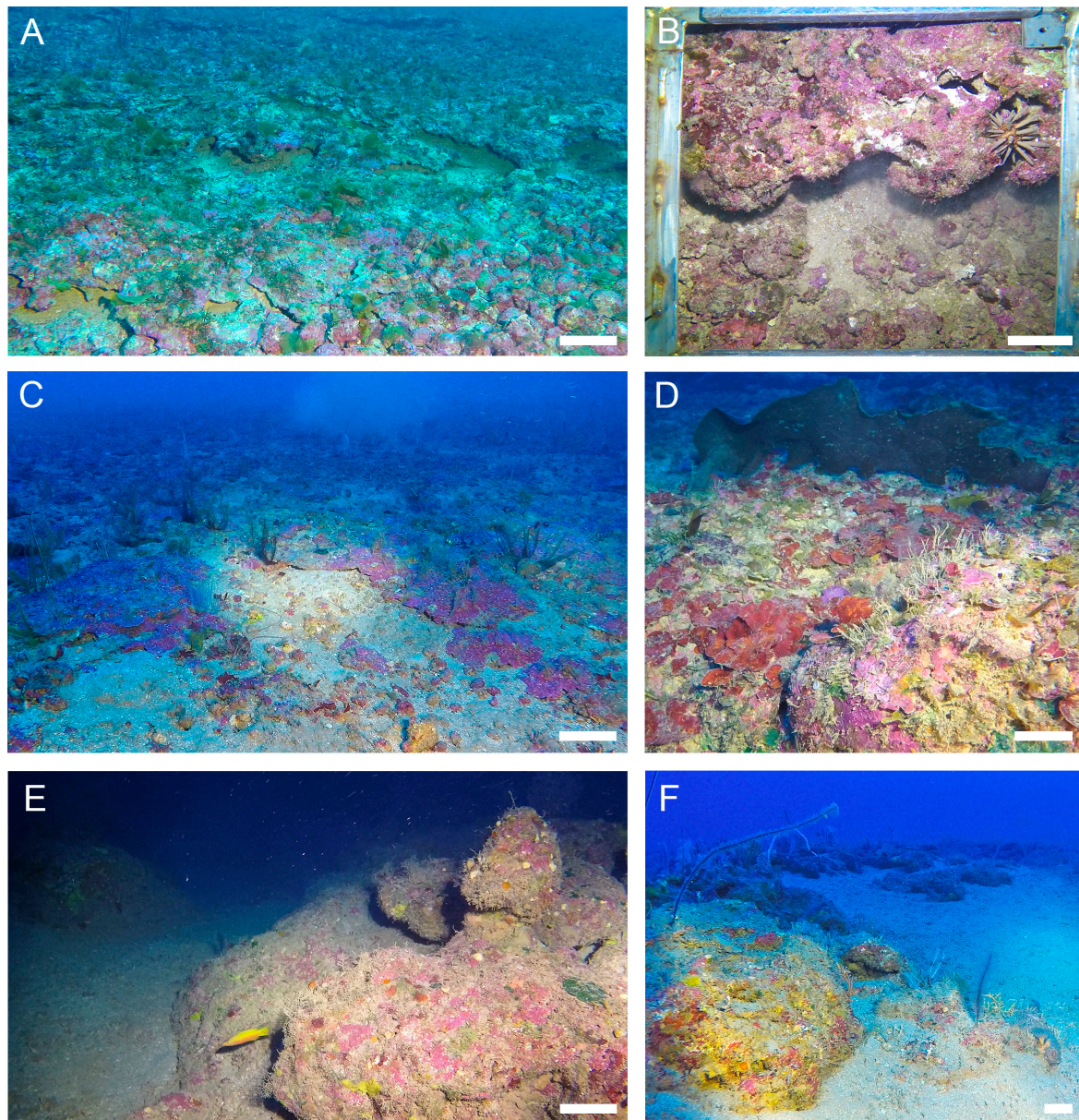


**Figure 8.** In situ images of carbonate concretions (A–D) and carbonate reefs (E–F) at different sampling sites/depths on the DRS (Table A1): (A) Transition from densely packed rhodoliths to carbonate concretions at S4 (63); (B) Detail of a concretion formation covered by CCA and *Peyssonnelia* sp. at S4 (63 m); (C) Carbonate concretions covered by CCA and *Peyssonnelia* spp. with crinoids at N5 (80 m); (D) Detail of carbonate concretions covered by CCA and *Peyssonnelia* spp. with the kelp *Laminaria abyssalis* at S1 (70 m); (E, F) Complex reef formations covered by CCA at S2 (103 m) and N2 (100 m), respectively. A, C, D, E, and F (lateral view); B (orthogonal view). Scale bar = 10 cm.

The third biogenic habitat was formed by carbonate concretions occupying sparse areas on the outer shelf (65–85 m depth) (Figures 6, 7 and 8A–D). Like the rhodoliths, the internal structure of these carbonate concretions is also formed mainly by CCA, *Peyssonnelia* spp., and Bryozoans in a multi-layer structure (Figure 9). By the analysis of in situ imagery and dredged material, these formations seem to develop from the stabilization of nodules and their latter cementation by calcifying organisms (e.g., CCA and Bryozoa), thus turning the rhodolith beds into gradual carbonate concretions. Several ledges were present at the border of the rhodolith beds to the carbonate concretions (Figure 8A–C).



**Figure 9.** Detail of rhodoliths (A–D) and carbonate concretions (E,F) showing laminar concentric arrangement with layers of CCA and Bryozoans, sampled from 54–70 m depth off the mouth of the Doce River and Costa das Algas Environmental Protected Area. Conspicuous brown fine sediments fill voids and cavities inside rhodoliths and carbonate concretions. Scale bar = 1 cm.

Rhodolith beds and calcareous concretions were usually formed by calcareous red algae (e.g., *Lithophyllum* spp. and *Peyssonnelia* spp.), with subordinated bryozoans (e.g., *Stylopoma hastata*). Vermetid gastropods and polychaete tubes were also recorded as secondary builders. These biogenic formations were filled with fine-grained brown sediment, which was observed trapped in cavities, voids, and borings (Figure 9).

The fourth and deeper biogenic habitat was higher relief reefs, reaching up to about 1.5 m high at 80–105 m depth. These reef formations were covered mainly by CCA, bryozoans, ascidians, and octocorals, building up substrate for other invertebrates (e.g., Echinoderms) and reef fishes

(Figure 8E–F). Due to sampling constraints, no dredged material was recovered from these reef formations. Yet, by the analysis of in situ imagery, not one single colony of scleractinian coral was observed, suggesting that the main builders were restricted to CCA and bryozoans, as recorded at the other shallower habitats in the region.

The most common coralline species on surfaces of rhodoliths from DRS was *Lithothamnion crispatum* Hauck. It is also among the most common rhodolith-forming coralline algae species in Brazil [6]. Other rhodolith-forming coralline species identified were: *Harveyolithon rupestre* (Foslie) A.Rösler, Perfectti, V.Peña and J.C.Braga, *Melyvonnea erubescens* (Foslie) Athanasiadis and D.L.Ballantine, *Lithophyllum prototypum* (Foslie) Foslie, *Titanoderma pustulatum* (J.V.Lamouroux) Nägeli, *Lithophyllum* sp., *Lithothamnion* sp. *Neogoniolithon brassica-florida* (Harvey) Setchell and L.R.Mason, *Phymatolithon* sp., and *Sporolithon amadoi* J.Richards and Bahia. Calcareous algae species from the order Peyssonneliales were also very common on rhodolith surfaces and carbonate concretions. The latter formation was also abundantly covered by *Lithothamnion* sp.

In this study, we have quantified the abundance (coverage) and density of CCA biogenic formations by mapping and comparing them across the depth range. Crustose coralline algae in both forms, rhodoliths and carbonate concretions, extended over a total area of about 1953 km<sup>2</sup> (≥10% cover) within the DRS (Figure 6A), with varying coverage along a latitudinal and depth gradient. Both CCA forms were abundant (≥50%) south and north of the Doce River mouth, while they had very low coverage (<10%) in front of the river mouth and to the north (Figure 6A). Rhodoliths predominated over carbonate concretions, occupying extensive continuous areas of about 1521 km<sup>2</sup> (Figure 6B). Carbonate concretions covered only 391 km<sup>2</sup>, being restricted to patchy deeper areas, usually closer to the continental shelf break (Figure 6C). Higher carbonate concretions coverage (≥50%) was recorded only in two small areas, one in the north and another in the south, from 65 to 105 m depth where RBs were usually present (Figure 6C). The distribution of the different biogenic formations (rhodoliths, carbonate concretions, and bryozoa) is shown in Figure 6D.

Crustose coralline percent cover (rhodoliths and carbonate concretions) differed among depths (PERMANOVA;  $F = 17.211$ ;  $p = 0.0002$ ; Figure 7A). The highest CCA abundance (mean ± SE;  $58 \pm 3\%$ ) was observed between depths of 66 and 75 m, while the lowest ( $16\% \pm 6\%$ ) was at the deepest waters below a depth of 96 m depth. Rhodolith percent cover also differed among depths (PERMANOVA;  $F = 15.805$ ,  $p = 0.0002$ ; Figure 7B). However, rhodolith abundance was highest at shallower depths than those of CCA concretion, between 46 and 65 m, while it was lowest deeper than 96 m. In addition, carbonate concretions also differed among depths (PERMANOVA;  $F = 28.315$ ;  $p = 0.0002$ ; Figure 7C) and presented the highest coverage ( $43\% \pm 4\%$ ) at the 66–75 m depth range, while it was virtually absent (about 0%) shallower than 55 m depth. Moreover, the density of rhodoliths also varied according to the depth gradient, similarly to rhodolith percent cover (PERMANOVA;  $F = 12.981$ ;  $p = 0.0002$ ; Figure 7D). The mean (± SE) highest density was  $92 \pm 6$  rhodoliths·m<sup>-2</sup> at 46–65 m depth, whereas the lowest was  $26 \pm 6$  rhodoliths·m<sup>-2</sup> at 66–95 m depth. The mean percent of dead rhodolith was about  $4.8\% \pm 0.5\%$  and did not differ among depths (PERMANOVA;  $F = 1.6812$ ;  $p = 0.0856$ ).

Overall, most rhodoliths were small (ca. 3 cm), but their mean diameter ranged from 1 to 12 cm (Figure 10). Their mean diameter differed according to depth (PERMANOVA;  $F = 18.347$ ;  $p = 0.0002$ ). The largest mean (± SD) diameter ( $4.6 \pm 1.5$  cm) was found at depths of 66 to 75 m while the smallest one ( $2.3 \pm 1.5$  cm) dominated at depths greater than 86 m. Moreover, most rhodoliths (42%) had mean diameters in the 2–4 cm size class. Only a few rhodoliths (about 0.2%) showed the largest size class (10–12 cm), while 16% represented the smallest one (0–2 cm). They had mostly boxwork (94%) and secondly praline morphologies (6%); they were also, for the majority, spheroidal to subspheroidal (Figure 11), representing 97% of the total rhodoliths collected from 50 to 65 m depth.

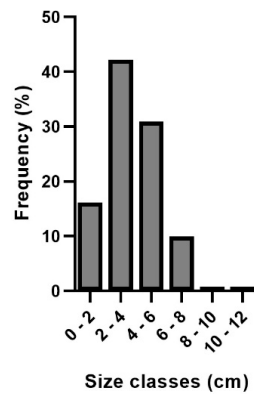


**Figure 10.** Mean diameter (cm) distribution of rhodoliths measured from different zones and depths of the DRS ( $n = \sim 2000$ ).

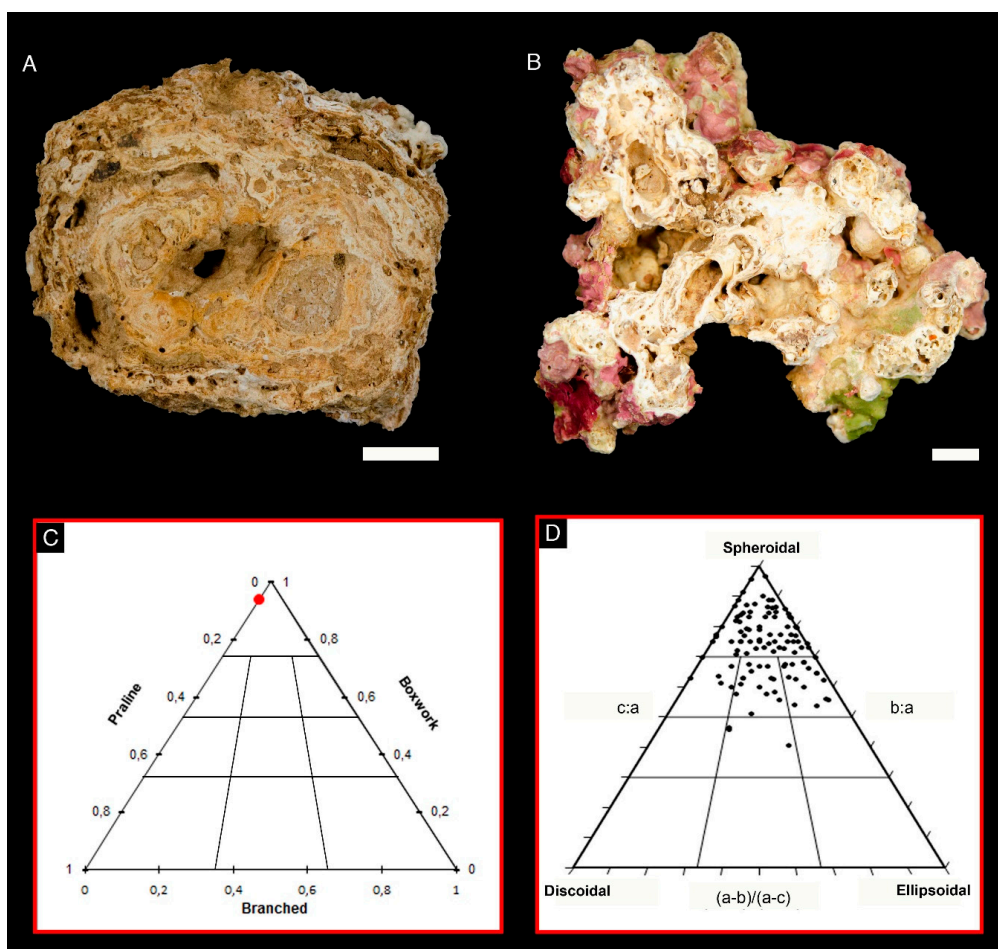


**Figure 11.** Characteristics of rhodoliths sampled at the DRS. (A) A spheroidal boxwork rhodolith; (B) an irregular to subspheroidal praline rhodolith; (C) TRIPLLOT of the main morphotypes, BW = boxwork, PR = pralines, BR = branches; (D) TRIPLLOT of the shape based on measurements of long (a), intermediate (b) and short (c) axes as described according to Bosence [4] and modified by Graham and Midgley [37]. Scale bar = 1 cm.

#### 4. Discussion

The dynamics of the suspended particulate material input at DRS will directly influence the distribution of bottom sediments. In general, fine sediments are abundant toward the north of the Doce River mouth [43]. Previous monitoring shows that the process of remobilization is normal for this

area and this material could be transported further due to its smaller granulometry. On the other hand, changes in sediment composition and size, as in the mining tailing material, will result in changes in the flocculation process and settling behavior, making them more likely to be dispersed by currents and waves and to reach greater distances [44].

The Doce River plume exerts a great influence through sedimentation in the spatial distribution of rhodoliths but also in its coverage and growth which might act together with other factors as depth, light intensity, and currents. The mean cover of rhodoliths at DRS was  $41.5\% \pm 1.7\%$  ( $\pm$ SE) considering coverage  $>10\%$ , which was lower than in the Abrolhos Bank ( $69.1\% \pm 1.7\%$ ; [10]). The rhodolith coverage recorded at 46 to 65 m depth at DRS was higher than that of shallower or deeper ones—36–45 m depth and  $>66$  m, respectively. RBs were almost absent at depths  $<35$  m, where sediments predominated. Fabricius and De'ath [45] found that CCA coverage in the Great Barrier Reef is related to sedimentation, being higher on reefs offshore with low sediment deposits. Because they are more distant from the coast, it is suggested that they suffer less influence from sedimentation, allowing for the greater penetration of light and providing more favorable conditions for CCA development in relation to the abundance and dimensions. On the other hand, at outer shelf sites, higher depths may become a CCA limiting growth factor (slowing their growth) once light penetration reduces concomitantly with deep increase [46]. In our study, the rhodoliths from 50 m depth were smaller ( $\sim 4$  cm) than those sampled at the south of ESCS (ca. 8 cm; [13]) or at the Abrolhos Bank (mean 6 cm; [14]) also due to sedimentation as observed by Brasileiro et al. [17] by analyzing their inner structure. Ultimately, the mean coverage and small size of rhodoliths at the study area may also result in a lower carbonate production than the Abrolhos Bank (estimated in  $1.0 \pm 0.7 \text{ kg m}^{-2} \text{ yr}^{-1}$ , [14]). In fact, rhodoliths in the Abrolhos Banks are located farther away from the coast and sediment inputs.

Rhodoliths at DRS showed an overall high vitality (mean 95%), whatever the depth, indicating minimum light conditions for CCA survival and/or their adaptation to restricted light ranges eventually faced at this region [47]. Moreover, the prevailing hydrodynamics along the ESCS is also considered as an important driver controlling the occurrence of these extensive beds and their vitality. Wave-dominated shelf, low sediment input, and a seasonal shelf upwelling [20,48] create favorable conditions for the development of extensive RBs. Upwelling along the DRS was also pointed out by many authors [49–51], which has been associated to the intrusion of the South Atlantic Central Water (SACW; [45]). Ovalle et al. [52] and Palóczy et al. [50] found that the temperature near the seabed was lower than  $21^\circ\text{C}$  in many points along the ESCS, pointing out qualitative evidences of the influence of the SACW at this region. This oceanographic circulation mechanism is probably one of the most important drivers, along with the sedimentation at this region, affecting the vitality of rhodoliths, at once contributing to the nutrient enrichment of the water and lowering its temperature.

Rhodoliths at DRS were more abundant in two discontinuous areas at depths between 45 and 65 m, occupying one extensive area south of the Doce River mouth encompassed by Costa das Algas Environmental Protection Area, as well as one smaller area at the south of the Abrolhos Shelf. North of the Doce River mouth, a very low rhodolith abundance ( $<10\%$ ) region extended about  $400 \text{ km}^2$  between the two previous areas (Figure 6B). The low coverage of rhodoliths might be a consequence of long-term deposition of fine sediments at the seafloor. At this area, carbonate concretions dominated the outer shelf at depth between 65 and 80 m. On the other hand, the region southward of the river mouth, which harbors two Marine Protected Areas, was also impacted by the plume but to a lesser extent [24]. At Costa das Algas Environmental Protected Area, we found the highest percent cover of rhodoliths deeper than 50 m ( $44.7 \pm 3.0$ ;  $\pm$ SE), at about 20 km away the coast, probably related to the lower terrigenous sedimentation [20] but also to resuspension processes by water motion in this area and its northward transport [53]. However, we found terrigenous sediments trapped on rhodoliths and carbonate concretions in this area. Following Brasileiro et al. [17] and Vieira et al. [32] and the results obtained herein, we can affirm that the Doce River sedimentation affected these habitats, however, we did not determine yet that these sediments originated from mining wastes. In contrast, at another MPA, Santa Cruz National Wildlife Refuge, rhodoliths were absent in shallower waters, probably due

to a high sedimentation regime from the local river Piraquê-Açu and low water motion. In this sense, it has been shown that reductions or discontinuities in shallow rhodoliths coincide with areas of low water motion and sedimentation or areas of high water motion [54]. In deep waters, currents and periodic storm waves may be sufficient to move rhodoliths [55]. In the Gulf of California, for example, rhodoliths are protected from smothering by fine sediments through tidal currents or waves [56].

Water motion is considered as one of the most important variables governing rhodolith occurrence and development as well as their shape and form [57]. Large boxwork rhodoliths grow under relatively calm conditions, with infrequent overturning [5,57]. The frequency of overturning of rhodoliths increases from the boxwork rhodoliths and reaches a maximum in the maerl facies (mainly unattached branches) and pralines [5]. Compact pralines and unattached branches do not undergo occasional burial by finer sediments, since their growth and periodical overturning keep up with the relatively low sedimentation rate [5]. Rhodolith shape, which can range from ellipsoidal to discoidal and spheroidal [4,5] also depends on overturning and water motion, mainly for ellipsoidal and discoidal forms [57].

The 10 rhodolith-forming coralline taxa recorded in this study are commonly found in near beds of Northeast and Southeast Brazil [6,58]. However, the number of species found in the area could be an underestimation, because it was based only on morpho-anatomy. Indeed, in the last 20 years, the traditional taxonomy has been integrated with molecular analysis that has revealed many cryptic species in coralline algae [59–61].

In the present work, we characterized the RBs and surrounding biogenic formations as bryozoans and reefs covered by CCA. Bryozoans were also found previously as the dominant group building the Abrolhos Bank pinnacles in Brazil [62]. Our study identified bryozoans as the main component between depths of 35 and 50 m on the DRS. CCA concretions were also spatially characterized at the outer shelf of the DRS. Basso et al. [63] first reported the occurrence of concretions of an irregularly domed shape on Espírito Santo shelf, as unequivocal evidence for coralline-driven substrate. Similar structures are typical in the Mediterranean Sea—named “coralligène”, they correspond to very complex biogenic structures mainly created by the outgrowth of encrusting calcareous algae on hard substrata in dim light conditions [64,65].

Rhodoliths have a higher abundance in the Costa das Algas Environmental Protection Area, playing an important ecological role for macroalgae and invertebrate settlement and colonization, enhancing the complexity of the local community and explaining why this area corresponds to one of the richest biodiversity marine environments of Brazil. However, these RBs as well as other biogenic formations are affected by the proximity to the river mouth and to increased river discharges as a result of poor management of the Doce River Basin, as in the case of the Mariana disaster and other human activities.

## 5. Conclusions

At DRS, RBs were more abundant in a large area at mid and outer shelf south of the Doce River mouth between depths of 45 and 65 m. This spatial distribution and coverage were most likely influenced by the river sedimentation and light. However, since there are no previous detailed studies on RBs along the DRS, we could not assess the impact of sedimentation of dam wastes on RBs' abundance and density. In any case, these are valuable results for the further monitoring of long-term effects. The determination of parameters such as abundance, shape, size, and vitality of rhodoliths proved to be of fundamental importance to assess the RBs. These data will also serve as a baseline for future monitoring studies, as well as for comparison with other priority areas for biodiversity conservation in RBs, such as the Abrolhos Bank.

Considering that the growth of these rhodoliths is slow compared to other tropical beds and considering their huge importance as that they constitute a substrate for a high diversity of associated organisms, this rhodolith bed area should receive special attention concerning its conservation and management. This includes further studies to better characterize the biodiversity in Costa das Algas

Environmental Protected Area and the ecological role of rhodoliths in relation to associated organisms. Biodiversity data associated with rhodoliths that will be incorporated in the next term of this project may help to demonstrate the great value of this area for marine conservation. Moreover, the implementation of a management and conservation plan for the Doce River Basin is necessary in order to preserve this ecosystem due to its influence in the region.

Recently, another important disaster was reported in August 2019, when an oil spill was first observed on Brazilian jurisdictional waters, affecting about 2250 km of coastline in northeastern Brazil. Several Brazilian researchers highlighted that RBs have been severely threatened and called for an urgent action to evaluate and mitigate the oil spill and to remediate and restore RB areas [66].

Finally, an increasing awareness about the importance of these benthic habitats in Brazil is needed to implement national initiatives to characterize them in different marine environmental conditions (e.g., shallow, deep, islands). This will allow researchers and managers to draw up an effective conservation strategy at the national scale, taking into account the several threats (e.g., mining wastes, oil spill) that these ecosystems face.

**Author Contributions:** Conceptualization, G.M.A.-F., R.G.B., V.L.H., C.S.K. and A.C.B.; methodology, G.M.A.-F., R.G.B., V.L.H., C.S.K., N.F.V., F.V.V., D.B.S. and F.C.M.; formal analysis, V.L.H., C.S.K. and D.B.S.; data curation, V.L.H. and F.V.V.; writing—original draft preparation, V.L.H., C.S.K., R.G.B.; writing—review and editing, V.L.H., C.S.K., R.G.B., F.C.M., A.C.B., L.T.S. and R.L.M.; project administration, A.C.B., G.M.A.-F., R.L.M., L.T.S.; funding acquisition, A.C.B., R.L.M. and G.M.A.-F. All authors have read and agreed to the published version of the manuscript.

**Funding:** Financial support was provided by: Conselho Nacional de Desenvolvimento Científico e Tecnológico (CNPq), Coordenação de Aperfeiçoamento de Pessoal de Nível Superior (CAPES), Fundação de Amparo à Pesquisa do Estado do Rio de Janeiro (FAPERJ), Fundação de Amparo à Pesquisa do Estado do Espírito Santo (FAPES), Rede Rio Doce Mar (Fundação Renova) and Agência Nacional do Petróleo, Gás Natural e Biocombustíveis/BRASOIL.

**Acknowledgments:** We thank Lais V. Ramalho (IPJBRJ) for Bryozoa taxonomic identification and Instituto Chico Mendes de Conservação da Biodiversidade (ICMBio) for research permits. Our deepest gratitude is to G.M.A.-F., who passed away, for his outstanding contribution to this paper. We also thank three anonymous reviewers for their valuable comments that greatly improved the manuscript.

**Conflicts of Interest:** The authors declare no conflict of interest.

## Appendix A

**Table A1.** Locations and depths of the study sites showing the habitat recorded by the images illustrated in Figures 3–5 and 8 (B = Bryozoa; CC = Carbonate Concretion; R = Reef; RB = Rhodolith Bed; S = Sediment).

Study Site	Zone	Habitat	Depth (m)	Latitude (S)	Longitude (W)
N1	North	B	50	19°28'9.30"	39°18'4.44"
N2	North	R	100	19°33'59.34"	39°4'2.35"
N3	North	RB	70	19°34'29.91"	39°9'33"
N4	North	RB	90	19°35'13.53"	39°8'30.74"
N5	North	CC	80	19°38'38.72"	39°20'32.96"
DR1	Doce River Mouth	S	60	19°41'1.33"	39°28'43.62"
DR2	Doce River Mouth	S	80	19°42'6.13"	39°25'57.87"
DR3	Doce River Mouth	RB	50	19°44'18.99"	39°32'20.7"
DR4	Doce River Mouth	S	68	19°45'8.94"	39°31'30.24"
DR5	Doce River Mouth	S	40	19°46'19.64"	39°40'51.31"
S1	South	CC	70	19°54'8.82"	39°41'2.12"
S2	South	R	103	19°53'50.6"	39°40'29.88"
S3	South	B	45	19°57'59.45"	39°55'1.25"
S4	South	RB/CC	63	19°59'9.68"	39°45'2.9"
S5	South	B	45	20°1'40.74"	39°57'42.74"
S6	South	S	100	20°1'4.92"	39°56'11.12"
S7	South	S/B	42	20°6'41.48"	39°59'47.4"
S8	South	B	49	20°9'26.62"	39°53'25.52"
S9	South	B	40	20°12'46.6"	40°3'10"

## References

1. Foster, M.S. Rhodoliths: Between rocks and soft places—Minireview. *J. Phycol.* **2001**, *37*, 659–667. [[CrossRef](#)]
2. Steller, D.L.; Riosmena-Rodríguez, R.; Foster, M.S.; Roberts, C.A. Rhodolith bed diversity in the Gulf of California: The importance of rhodolith structure and consequences of disturbance. *Aquat. Conserv. Mar. Freshw. Ecosyst.* **2003**, *13*, S5–S20. [[CrossRef](#)]
3. Basso, D.; Babbini, L.; Kaleb, S.; Bracchi, V.A.; Falace, A. Monitoring deep Mediterranean rhodolith beds. *Aquatic. Conserv. Mar. Freshw. Ecosyst.* **2016**, *26*, 549–561. [[CrossRef](#)]
4. Bosence, D.W.J. Description and classification of rhodoliths (rhodoids, rhodolites). In *Coated Grains*; Peryt, T.M., Ed.; Springer: Berlin/Heidelberg, Germany, 1983; pp. 217–224.
5. Basso, D. Deep rhodolith distribution in the Pontian Islands, Italy: A model for the paleoecology of a temperate sea. *Palaeogeogr. Palaeoclimatol. Palaeoecol.* **1998**, *137*, 173–187. [[CrossRef](#)]
6. Amado-Fiho, G.M.; Bahia, R.G.; Pereira-Filho, G.H.; Longo, L.L. South Atlantic rhodolith beds: Latitudinal distribution, species composition, structure and ecosystem functions, threats and conservation status. In *Rhodolith/Maërl Beds: A Global Perspective*; Riosmena-Rodríguez, R., Nelson, W., Aguirre, J., Eds.; Springer International Publishing: Geerbestrasse, Switzerland, 2017; pp. 299–317.
7. Martin, S.; Gattuso, J.P. Response of Mediterranean coralline algae to ocean acidification and elevated temperature. *Glob. Chang. Biol.* **2009**, *15*, 2089–2100. [[CrossRef](#)]
8. Martin, S.; Coahu, S.; Vignot, C.; Zimmerman, G.; Gattuso, J.P. One-year experiment on the physiological response of the Mediterranean crustose coralline alga, *Lithophyllum cabiochae*, to elevated pCO<sub>2</sub> and temperature. *Ecol. Evol.* **2013**, *3*, 676–693. [[CrossRef](#)]
9. Ragazzola, F.; Foster, L.C.; Form, A.U.; Büscher, J.; Hansteen, T.H.; Fietzke, J. Phenotypic plasticity of coralline algae in a high CO<sub>2</sub> world. *Ecol. Evol.* **2013**, *3*, 3436–3446.
10. Blake, C.; Maggs, C.A. Comparative growth rates and internal banding periodicity of maerl species (Corallinales, Rhodophyta) from northern Europe. *Phycologia* **2003**, *42*, 606–612. [[CrossRef](#)]
11. Nelson, W.A. Calcified macroalgae—Critical to coastal ecosystem and vulnerable to change: A review. *Mar. Freshw. Res.* **2009**, *60*, 781–801. [[CrossRef](#)]
12. McCoy, S.J.; Kamenos, N.A. Coralline algae (Rhodophyta) in a changing world: Integrating ecological, physiological and geochemical responses to global change. *J. Phycol.* **2015**, *51*, 6–24. [[CrossRef](#)]
13. Amado-Filho, G.M.; Maneveldt, G.W.; Pereira-Filho, G.H.; Manso, R.C.C.; Bahia, R.G.; Barros-Barreto, M.B.; Guimarães, S.M.P.B. Seaweed Diversity Associated with a Brazilian Tropical Rhodolith Bed. *Cienc. Mar.* **2010**, *36*, 371–391. [[CrossRef](#)]
14. Amado-Filho, G.M.; Moura, R.L.; Bastos, A.C.; Salgado, L.T.; Sumida, P.Y.; Guth, A.Z.; Francini-Filho, R.B.; Pereira-Filho, G.H.; Abrantes, D.P.; Brasileiro, P.S.; et al. Rhodolith beds are major CaCO<sub>3</sub> bio-factories in the tropical south west atlantic. *PLoS ONE* **2012**, *7*, e35171. [[CrossRef](#)] [[PubMed](#)]
15. Amado-Filho, G.M.; Pereira-Filho, G.H.; Bahia, R.G.; Abrantes, D.P.; Veras, P.C.; Matheus, Z. Occurrence and distribution of rhodolith beds on the Fernando de Noronha Archipelago of Brazil. *Aquat. Bot.* **2012**, *101*, 41–45. [[CrossRef](#)]
16. Cavalcanti, G.S.; Gregoraci, G.B.; Santos, E.O.; Silveira, C.B.; Meirelles, P.M.; Longo, L.; Gotoh, K.; Naramura, S.; Iida, T.; Sawabe, T.; et al. Physiologic and metagenomic attributes of the rhodoliths forming the largest CaCO<sub>3</sub> bed in the South Atlantic Ocean. *ISME J.* **2014**, *8*, 52–62. [[CrossRef](#)]
17. Brasileiro, P.S.; Braga, J.C.; Amado-Filho, G.M.; Leal, R.N.; Bassi, D.; Franco, T.; Bastos, A.C.; Moura, R. Burial rate determines Holocene rhodolith development on the Brazilian Shelf. *Palaios* **2018**, *33*, 464–477. [[CrossRef](#)]
18. Vale, N.F.; Amado-Filho, G.M.; Braga, J.C.; Brasileiro, P.S.; Karez, C.S.; Moraes, F.C.; Bahia, R.G.; Bastos, A.C.; Moura, R.L. Structure and composition of rhodoliths from the Amazon River mouth, Brazil. *J. S. Am. Earth Sci.* **2018**, *84*, 149–159. [[CrossRef](#)]
19. Moura, R.M.; Amado-Filho, G.M.; Moraes, F.C.; Brasileiro, P.S.; Salomon, P.S.; Mahiques, M.M.; Bastos, A.C.; Almeida, M.G.; Silva, J.M.; Araujo, B.F.; et al. An extensive reef system at the Amazon River mouth. *Sci. Adv.* **2016**, *2*, e1501252. [[CrossRef](#)]
20. Bastos, A.C.; Quaresma, V.S.; Marangoni, M.B.; D’Agostini, D.P.; Bourguignon, S.N.; Cetto, P.H.; Silva, A.E.; Amado-Filho, G.M.; Moura, R.L.; Collins, M. Shelf morphology as an indicator of sedimentary regimes: A synthesis from a mixed siliclastic carbonate shelf on the eastern Brazilian margin. *J. S. Am. Earth Sci.* **2015**, *63*, 125–136. [[CrossRef](#)]

21. Berlandi, R.M.; Figueiredo, M.A.O.; Paiva, P.C. Rhodolith morphology and the diversity of polychaetes off the southeastern Brazilian coast. *J. Coast. Res.* **2012**, *28*, 280–287. [[CrossRef](#)]
22. Dias, G.T.M.; Villaça, R.C. Coralline algae depositional environments on the Brazilian Central-South-Eastern shelf. *J. Coast. Res.* **2012**, *28*, 270–279. [[CrossRef](#)]
23. Marins, B.V.; Amado-Filho, G.M.; Barreto, M.B.B.; Longo, L.L. Taxonomy of the southwestern Atlantic endemic kelp: *Laminaria abyssalis* and *Laminaria brasiliensis* (Phaeophyceae, Laminariales) are not different species. *Phycol. Res.* **2012**, *60*, 51–60. [[CrossRef](#)]
24. Magris, R.A.; Marta-Almeida, M.; Monteiro, J.A.F.; Ban, N.C. A modelling approach to assess the impact of land mining on marine biodiversity: Assessment in coastal catchments experiencing catastrophic events (SW Brazil). *Sci. Total. Environ.* **2019**, *659*, 828–840. [[CrossRef](#)] [[PubMed](#)]
25. Gomes, L.E.O.; Correa, L.B.; Sá, F.; Rodrigues-Neto, R.; Bernardino, A.F. The impacts of the Samarco mine tailing spill on the Rio Doce estuary, Eastern Brazil. *Mar. Pollut. Bull.* **2017**, *120*, 28–36. [[CrossRef](#)] [[PubMed](#)]
26. Golder. *Avaliação do Estado de Conservação dos Bancos de Rodolitos Adjacentes à Foz do Rio Doce*; Report prepared for Samarco Mineração S.A.; Golder Associates Ltda: Rio de Janeiro, Brazil, 2016; p. 46.
27. Oliveira, K.S.S.; Quaresma, V.S. Temporal variability in the suspended sediment load and streamflow of the Doce River. *J. S. Am. Earth Sci.* **2017**, *78*, 101–115. [[CrossRef](#)]
28. Quaresma, V.S.; Catabriga, G.; Bourguignon, S.N.; Godinho, E.; Bastos, A.C. Modern sedimentary processes along the Doce river adjacent continental shelf. *Brazilian J. Geol.* **2015**, *45*, 635–644. [[CrossRef](#)]
29. Guimarães, S.M.P.B. Uma análise da diversidade da flora marinha bentônica do Estado do Espírito Santo, Brasil. *Hoehnea* **2003**, *30*, 11–19.
30. Guimarães, S.M.P.B. A revised checklist of benthic marine Rhodophyta from the State of Espírito Santo, Brazil. *Boletim do Instituto de Botânica* **2006**, *17*, 143–194.
31. Horta, P.A.; Amancio, E.; Coimbra, C.S.; Oliveira, E.C. Considerações sobre a distribuição e origem da flora de macroalgas marinhas brasileiras. *Hoehnea* **2001**, *28*, 243–265.
32. Vieira, F.; Bastos, A.C.; Quaresma, V.S.; Leite, M.D.; Costa A., Jr.; Oliviera, K.S.S.; Dalvi, C.; Bahia, R.G.; Holz, V.L.; Moura, R.L.; et al. Along-shelf changes in mixed carbonate-siliciclastic sedimentation patterns. *Cont. Shelf Res.* **2019**, *187*, 1039642. [[CrossRef](#)]
33. Kohler, K.E.; Gill, S.M. Coral Point Count with Excel extensions (CPCe): A Visual Basic program for the determination of coral and substrate coverage using random point count methodology. *Comput. Geosci.* **2006**, *32*, 1259–1269. [[CrossRef](#)]
34. Bahia, R.G.; Abrantes, D.P.; Brasileiro, P.S.; Amado-Filho, G.M.; Pereira-Filho, G.H. Rhodolith bed structure along a depth gradient on the northern coast of Bahia state, Brazil. *Brazilian J. Oceanogr.* **2010**, *58*, 323–337. [[CrossRef](#)]
35. Abramoff, M.D.; Magalhaes, P.; Ram, S.J. Image Processing with ImageJ. *Biophotonics Int.* **2004**, *11*, 36–42.
36. Bosence, D.W.J.; Pedley, H.M. Sedimentology and palaeoecology of Miocene coralline algal biostrome from the Maltese Islands. *Palaeogeog. Palaeoclim. Palaeoecol.* **1982**, *38*, 9–43. [[CrossRef](#)]
37. Graham, D.J.; Midgley, N.G. Graphical representation of particle shape using triangular diagrams: An Excel spreadsheet method. *Earth Surf. Process. Landf.* **2000**, *25*, 1473–1477. [[CrossRef](#)]
38. Basso, D.; Nalin, R.; Nelson, C.S. Shallow-water *Sporolithon* rhodoliths from North Island (New Zealand). *Palaios* **2009**, *24*, 92–103. [[CrossRef](#)]
39. Maneveldt, G.W.; van der Merwe, E. *Heydrichia cerasina* sp. nov. (Sporolithales, Corallinophycidae, Rhodophyta) from the southernmost tip of Africa. *Phycologia* **2012**, *51*, 11–21. [[CrossRef](#)]
40. Bahia, R.G. Algas Coralináceas Formadoras de Rodolitos da Plataforma Continental Tropical e Ilhas Oceânicas do Brasil: Levantamento Florístico e Taxonomia. Ph.D. Thesis, Escola Nacional de Botânica Tropical, Rio de Janeiro, Brazil, 2014.
41. Clarke, K.R. Non-parametric multivariate analyses of changes in community structure. *Aust. J. Ecol.* **1993**, *18*, 117–143. [[CrossRef](#)]
42. Anderson, M.J.; Gorley, R.N.; Clarke, K.R. *Permanova+ for Primer: Guide to Software and Statistical Methods*; Primer-E: Plymouth, UK, 2008.
43. Bastos, A.C.; Oliveria, K.S.S.; Fernandes, L.F.; Pereira, J.B.; Demoner, L.E.; Neto, R.R.; Costa, E.S.; Sá, F.; Silva, C.A.; Lerhback, B.D.; et al. *Monitoramento da Influência da Pluma do Rio Doce após o Rompimento da Barragem de Rejeitos em Mariana/MG, Novembro de 2015: Processamento, Interpretação e Consolidação de Dados*; Universidade Federal do Espírito Santo: Vitoria, Brasil, 2017; p. 254.

44. Grilo, C.F.; Quaresma, V.S.; Amorim, G.F.L.; Bastos, A.C. Changes in flocculation patterns of cohesive sediments after an iron ore mining dam failure. *Mar. Geol.* **2018**, *400*, 1–11. [[CrossRef](#)]
45. Fabricius, K.; D'each, G. Environmental factors associated with the spatial distribution of crustose coralline algae on the Great Barrier Reef. *Coral Reefs* **2001**, *19*, 303–309. [[CrossRef](#)]
46. Tâmega, F.T.S.; Bassi, D.; Figueiredo, M.A.O.; Cherkinsky, A. Deep-water rhodolith bed from central Brazilian continental shelf, Campos Basin: Coralline algal and faunal taxonomic composition. *Galaxea* **2014**, *16*, 21–31. [[CrossRef](#)]
47. Figueiredo, M.A.O.; Coutinho, R.; Villas-Boas, A.B.; Tâmega, F.T.S.; Mariath, R. Deep-water rhodolith productivity and growth in the southwestern Atlantic. *J. Appl. Phycol.* **2012**, *24*, 487–493. [[CrossRef](#)]
48. Marins, B.V.; Amado-Filho, G.M.; Barbarino, E.; Pereira-Filho, G.H.; Longo, L.L. Seasonal changes in population structure of the tropical deep-water kelp *Laminaria abyssalis*. *Phycol. Res.* **2014**, *62*, 55–62.
49. Mazzini, P.L.F.; Barth, J.A. A comparison of mechanisms generating vertical transport in the Brazilian coastal upwelling regions. *J. Geophys. Res. Ocean.* **2013**, *118*, 5977–5993. [[CrossRef](#)]
50. Palóczy, A.; Brink, K.H.; Silveira, I.C.A.; Arruda, W.Z.; Martins, R.P. Pathways and mechanisms of offshore water intrusions on the Espírito Santo Basin shelf (18° S–22° S, Brazil). *J. Geophys. Res. Ocean.* **2016**, *121*, 5134–5163. [[CrossRef](#)]
51. Pereira, A.F.; Belem, A.L.; Castro, B.M.; Geremias, R. Tide–topography interaction along the eastern Brazilian shelf. *Cont. Shelf Res.* **2005**, *25*, 1521–1539. [[CrossRef](#)]
52. Ovalle, A.R.C.; Resende, C.E.; Carvalho, C.E.V.; Jennerjahn, T.C.; Ittekkot, V. Biogeochemical characteristics of coastal waters adjacent to small river-mangrove systems, East Brazil. *Geo. Mar. Lett.* **1999**, *19*, 179–185. [[CrossRef](#)]
53. Rudorff, N.; Rudorff, C.N.; Kampel, M.; Ortiz, G. Remote sensing monitoring of the impact of a major mining wastewater disaster on the turbidity of the Doce River plume off the eastern Brazilian coast. *ISPRS J. Photogramm. Remote Sens.* **2018**, *145*, 349–361. [[CrossRef](#)]
54. Marrack, E.C. The relationship between water motion and living rhodolith beds in the southwestern Gulf of California, Mexico. *Palaeos* **1999**, *14*, 159–171. [[CrossRef](#)]
55. Harris, P.T.; Tsuji, Y.; Marshall, J.F.; Davies, P.J.; Honda, N.; Matsuda, H. Sand and rhodolith-gravel entrainment on the mid- to outer-shelf under a western boundary current: Fraser Island continental shelf, eastern Australia. *Mar. Geol.* **1996**, *129*, 313–330. [[CrossRef](#)]
56. Halfar, J.; Eisele, M.; Riegl, B.; Hetzinger, S.; Godinez-Orta, L. Modern Rhodolith dominated carbonates at Punta Chivato, Mexico. *Geodiversitas* **2012**, *34*, 99–113. [[CrossRef](#)]
57. Bracchi, V.A.; Angeletti, L.; Marchese, F.; Taviani, M.; Cardone, F.; Hajdas, I.; Grande, V.; Prampolini, M.; Caragnano, A.; Corselli, C.; et al. A resilient deep-water rhodolith bed off the Egadi Archipelago (Mediterranean Sea) and its actuopaleontological significance. *Alp. Mediterr. Quat.* **2019**, *32*, 1–20.
58. Brasileiro, P.; Pereira-Filho, G.; Bahia, R.; Abrantes, D.; Guimarães, S.; Moura, R.; Francini-Filho, R.; Bastos, A.; Amado-Filho, G. Macroalgal composition and community structure of the largest rhodolith beds in the world. *Mar. Biodivers.* **2016**, *46*, 407–420. [[CrossRef](#)]
59. Sissini, M.N.; Oliveira, M.C.; Gabrielson, P.W.; Robinson, N.M.; Okolodkov, Y.B.; Riosmena-Rodríguez, R.; Horta, P.A. *Mesophyllum erubescens* (Corallinales, Rhodophyta)—So many species in one epithet. *Phytotaxa* **2014**, *190*, 299–319. [[CrossRef](#)]
60. Hernandez-Kantun, J.J.; Gabrielson, P.W.; Hughey, J.R.; Pezolesi, L.; Rindi, F.; Robinson, N.M.; Peña, V.; Riosmena-Rodríguez, R.; le Gall, L.; Adey, W.H. Reassessment of branched *Lithophyllum* spp. (Corallinales, Rhodophyta) in the Caribbean Sea with global implications. *Phycologia* **2016**, *55*, 619–639. [[CrossRef](#)]
61. Richards, J.L.; Sauvage, T.; Schmidt, W.E.; Fredericq, S.; Hughey, J.R.; Gabrielson, P.W. The coralline genera *Sporolithon* and *Heydrichia* (Sporolithales, Rhodophyta) clarified by sequencing type material of their genotypes and other species. *J. Phycol.* **2017**, *53*, 1044–1059. [[CrossRef](#)]
62. Bastos, A.C.; Moura, R.L.; Moraes, F.C.; Vieira, L.S.; Braga, J.B.; Ramalho, L.V.; Amado-Filho, G.M.; Magdalena, U.R.; Webster, J.M. Bryozoans are major modern builders of South Atlantic oddly shaped reefs. *Sci. Rep.* **2018**, *8*, 9638. [[CrossRef](#)]
63. Basso, D.; Tavares de Macedo, D.G.; Henriques, M.C. The occurrence of coralligène de plateau in Brazilian coastal waters. In Proceedings of the IV International Rhodolith Workshop, Granada, Spain, 17–21 September 2012.

64. Ballesteros, E. Mediterranean coralligenous assemblages: A synthesis of present knowledge. *Oceanogr. Mar. Biol.* **2006**, *44*, 123–195.
65. Martin, C.S.; Giannoulaki, M.; Leo, F.; Scardi, M.; Salomidi, M.; Knittweis, L.; Pace, M.L.; Garofalo, G.; Gristina, M.; Ballesteros, E.; et al. Coralligenous and maërl habitats: Predictive modelling to identify their spatial distributions across the Mediterranean Sea. *Sci. Rep.* **2014**, *4*, 5073. [[CrossRef](#)]
66. Sissini, M.N.; Berchez, F.; Hall-Spencer, J.; Ghilardi-Lopes, N.; Carvalho, V.F.; Schubert, N.; Koerich, G.; Diaz-Pulido, G.; Silva, J.; Serrão, E.; et al. Brazil oil spill response: Protect rhodolith beds. *Science* **2020**, *367*, 156.



© 2020 by the authors. Licensee MDPI, Basel, Switzerland. This article is an open access article distributed under the terms and conditions of the Creative Commons Attribution (CC BY) license (<http://creativecommons.org/licenses/by/4.0/>).